Journal of the Association of Arab Universities for Basic and Applied Sciences (2015) **17**, 57–65

University of Bahrain

Journal of the Association of Arab Universities for Basic and Applied Sciences

www.elsevier.com/locate/jaaubas
www.sciencedirect.com

تحضير حفازات حمضية صلبة نصف مسامية من نوع MCM-48 متضمنة على الزركون ونشاطها التحفيزي للالكلة الفينول مع ثالثي بوتيل كحول

Tingshun Jiang, Yan Ma, Jinlian Cheng, Wangping Liu, Xuping Zhou, Qian Zhao*, Hengbo Yin

School of Chemistry and Chemical Engineering, Jiangsu University, Xuefu Road 301#, Zhenjiang 212013, PR China

الملخص:

تم تحضير حفازات حمضية صلبة نصف مسامية من نوع MCM-48 متضمنة على الزركون وبنسب مولارية مختلفة من السيلكون والزركون وذلك عن طريق معالجتها بمحلول حمض الكبريت ومحلول نترات النشادر على التوالي. وتم تعيين خواصها الفيزيوكيماوية بواسطة مطياف حيود الاشعة السينية وجهاز المجهر الالكتروني الناقل وجهاز الامتزاز العكسي – مجس النشادر المبرمج حرارياً وجهاز امتزاز – مجس النيتروجين. تم استقصاء الأداء الحفزي لهذه الحفازات باستعمال تفاعل ألكلة الفينول مع الكحول رباعي البيوتيل كتفاعل منشود. كشفت النتائج بأن حفاز ZrMCM-48/ $SO4^{-2}$ وحفاز H-ZrMCM-48 لا زالا يحتفظان بالبنية نصف المسامية المكعبة ل MCM-48 بالرغم من أن الترتيب نصف المسامي اصبح أقل.

بالمقارنة تحت الظروف المشابهة، فإن النشاط الحفزي لحفاز $SO4^{-2}$/ZrMCM-48(25) الحمضي الصلب هو الأعلى من بين كل الحفازات الأخرى. كذلك فإن درجة حرارة التفاعل المتدنية هي مناسبة لتكون 2,4-DTBP وبالمقابل فإن درجة حرارة التفاعل المرتفعة هي مناسبة لتكون 4-TBP.

Journal of the Association of Arab Universities for Basic and Applied Sciences (2015) **17**, 57–65

University of Bahrain

Journal of the Association of Arab Universities for Basic and Applied Sciences

www.elsevier.com/locate/jaaubas
www.sciencedirect.com

ORIGINAL ARTICLE

Preparation of mesoporous zirconium incorporated MCM-48 solid acid catalyst and its catalytic activity for alkylation of phenol with *tert*-butyl alcohol

Tingshun Jiang, Yan Ma, Jinlian Cheng, Wangping Liu, Xuping Zhou, Qian Zhao *, Hengbo Yin

School of Chemistry and Chemical Engineering, Jiangsu University, Xuefu Road 301#, Zhenjiang 212013, PR China

Received 24 June 2013; revised 26 November 2013; accepted 14 January 2014
Available online 4 February 2014

KEYWORDS

Mesoporous solid acid catalyst;
SO_4^{2-}/ZrMCM-48;
H-ZrMCM-48;
Alkylation;
Catalytic activity

Abstract Zirconium incorporated mesoporous MCM-48 solid acid catalysts with the different Si/Zr molar ratios were prepared by modification with H_2SO_4 and NH_4NO_3 solution, respectively. Their physicochemical properties were characterized by XRD, TEM, NH_3–TPD and N_2 physical adsorption. The catalytic performances of these catalysts were investigated by using the alkylation reaction of phenol and *tert*-butyl alcohol as the target reaction. The results reveal that the SO_4^{2-}/ZrMCM-48 and H-ZrMCM-48 catalysts still maintained the cubic mesporous structure of MCM-48, but the mesoporous ordering decreased. Under comparable conditions, the catalytic activity of SO_4^{2-}/ZrMCM-48(25) solid acid catalyst is the highest among all catalysts. The lower reaction temperature is favorable for formation of the 2,4-DTBP and the 4-TBP is easily formed at the higher reaction temperature.

1. Introduction

Alkylation of phenol with *tert*-butyl alcohol, an interesting industrial organic reaction, has received great interest due to its industrial and academic relevance (Dapurkar and Selvam, 2003; Huang et al., 2006). The butylated phenols like 2-t-butyl phenol (2-TBP), 4-t-butyl phenol (4-TBP) and 2, 4-di-t-butyl phenol (2,4-DTBP) are widely used as starting materials or important intermediates in some areas such as phenol resins, petrochemicals, fine chemicals, antioxidants, rubber chemicals, heat stabilizers of polymeric materials and agrochemical (Mathew et al., 2004; Ojha et al., 2005; Gui et al., 2008). Conventional, alkylation of phenol with *tert*-butyl alcohol were carried out by homogeneous liquid acid catalysts including sulfuric acid, phosphoric acid and hydrofluoric acid. However, several problems have emerged along with the use of these acid catalysts: increasing waste disposal costs, environmental non-friendliness,

* Corresponding author. Tel./fax: +86 (0)511 88791800.
E-mail address: qianzhao@mail.ujs.edu.cn (Q. Zhao).
Peer review under responsibility of University of Bahrain.

1815-3852 © 2014 Production and hosting by Elsevier B.V. on behalf of University of Bahrain.
http://dx.doi.org/10.1016/j.jaubas.2014.01.003

corrosiveness and low reaction selectivity (Elavarasan et al., 2011; Li et al., 2009; Ronchin et al., 2012; Yadav and Pathre, 2006). This greatly limits their industrial applications. Thus, some efforts to replace traditional homogeneous liquid acid catalysts by novel heterogeneous solid acid ones have been made due to some advantages of these solid acid catalysts such as high reactivity, no corrosion, environmental friendliness, easy handling, inexpensive and easy to recover and reuse (Chen et al., 2007; Jiang et al., 2008; Sohn et al., 2006).

Recently, many efforts for the target reaction were carried out by environmentally friendly heterogeneous solid acid catalysts such as cation-exchanged resins, zeolite, clay-based catalysts and mesoporous molecular sieves due to societal, environmental and economic pressure (Badamali et al., 2000; Chandra and Sharma, 1993; Dumitriu and Hulea, 2003; Krishnan et al., 2002; Subrahmanyam et al., 2005). Among solid acid catalysts, cation-exchanged resins exhibit good performance, but they are thermally unstable at higher reaction temperature. Microporous zeolites are usually regarded as the environmentally friendly catalysts because of their high acidity, highly thermal stability and easy separation from reaction products (Anand et al., 2003; Zhao et al., 2006). However, these microporous materials possess small pore size (< 2 nm), which severely limited the formation of butylated products like 2,4-DTBP.

M41S family mesoporous materials, discovered in 1992 (Kresge et al., 1992), have some potential applications in the fields of catalysis, adsorption, materials science and petrochemical industry owing to their high surface areas and tunable pore diameters (Du et al., 2011; Subashini and Pandurangan, 2007). Recently, the catalytic activities of some mesoporous solid acid catalysts have been evaluated by *t*-butylation of phenol (Savidha et al., 2004; Vinu et al., 2004) and the experimental results reveal that mesoporous solid acid catalyst is more ideal one for *t*-butylation of phenol as compared with the other solid acid catalysts like cation-exchange resin and microporous material. However, many of the previous reports focused on the study on mesoporous MCM-41 solid acid catalysts. Little attention is paid to investigation on mesoporous MCM-48 solid acid catalysts. Compared with the one-dimensional channel structure of MCM-41, MCM-48 was found to be a more potent and interesting candidate as catalyst or catalyst support due to its attractive and unique cubic arrangement of three-dimensional interwoven structure (Zhao et al., 2010a).

In this paper, we prepared several SO_4^{2-}/ZrMCM-48 and H-ZrMCM-48 solid acid catalysts by the impregnation method. The catalytic performances of these solid acid catalysts were investigated by the alkylation of phenol with *tert*-butyl alcohol. Among the four solid acid catalysts, we found that the SO_4^{2-}/ZrMCM-48(25) catalyst is the most promising and gives the highest phenol conversion under the comparable conditions.

2. Experimental

2.1. Materials

The chemicals used in this work were tetraethyl orthosilicate (TEOS) as a silica source, zirconium sulfate ($Zr(SO_4)_2{\cdot}4H_2O$) as Zr source, cetyltrimethyl ammonium bromide (CTAB) as a surfactant, respectively, and sodium hydroxide (NaOH), sodium fluoride (NaF), concentrated sulfuric acid (H_2SO_4), ammonium nitrate(NH_4NO_3), phenol and *tert*-butyl alcohol. All chemicals were of analytical grade and they are purchased from Shanghai Chemical Reagent Corporation, PR China.

2.2. Synthesis of Zr incorporated MCM-48 mesoprous molecular sieves

A detailed synthesis procedure for Zr incorporated MCM-48 mesoporous molecular sieve has been reported in our previous publication (Jiang et al., 2011). The typical composition for the synthesis of Zr incorporated MCM-48 was: 1TEOS: x Zr: 0.65CTAB: 0.5NaOH: 0.1NaF: $62H_2O$ ($x = 0.02$ and 0.04, respectively). The calcined samples were designated as ZrMCM-48(x), where x is the molar ratio of Si/Zr in synthesis gel.

2.3. Preparation of SO_4^{2-}/ZrMCM-48 solid acid catalysts

SO_4^{2-}/ZrMCM-48 solid acid catalysts were prepared by the wet impregnation method. Typically, 2 g of the calcined ZrMCM-48 sample was dissolved in 0.4 mol/L of H_2SO_4 solution with stirring for 1 h. The obtained suspension was statically placed at ambient temperature for 8 h till the suspension was deposited. After evaporating the solvent, the residual solid was dried at 100 °C for 12 h in an oven. The dried sample was calcined at 550 °C for 3 h in air at a heating rate of 2 °C/min, and denoted as SO_4^{2-}/ZrMCM-48(25) and SO_4^{2-}/ZrMCM-48(50).

2.4. Preparation of H-ZrMCM-48 solid acid catalyst (Sakthivel et al., 2003)

The calcined ZrMCM-48 samples were converted into acidic form by repeated ion exchange with 1 mol/L NH_4NO_3 solution at 80 °C with stirring for 1 h, followed by calcination at 550 °C for 6 h in air, and the protonated form was obtained, denoted as H-ZrMCM-48(25) and H-ZrMCM-48(50). For comparison, the H-MCM-48 and H-Y catalysts were prepared in the same manner.

2.5. Thermal and hydrothermal treatment of ZrMCM-48 sample

Thermal stability test, 1 g of calcined ZrMCM-48(50) sample was calcined again at different temperatures (700 and 800 °C) for 4 h in air, respectively. The obtained samples were designated as ZrMCM-48(50)-700 and ZrMCM-48(50)-800, correspondingly.

Hydrothermal stability test, 1 g of the ZrMCM-48(50) sample was respectively added into a 100 ml Teflon-lined stainless autoclave containing 80 ml of H_2O and hydrothermally treated at 100 °C for different times (12, 24 and 48 h). After this treatment, the hydrothermally treated sample was subsequently filtered and dried in an oven at 120 °C. The hydrothermal treated samples were denoted as ZrMCM-48(50)-12 h, ZrMCM-48(50)-24 h and ZrMCM-48(50)-48 h.

2.6. Characterization

XRD patterns were recorded on a powder XRD instrument (Rigaku D/max 2500PC) with Cu K_α radiation ($\lambda = 0.154$ 18 nm) operating at 40 kV and 50 mA in the 2θ range of

1–10°. N_2 adsorption–desorption isotherms at 77 K were recorded with a NOVA2000e analytical system made by Quantachrome Corporation (USA). Prior to measurement, all samples were outgassed at 300 °C for 3 h. The specific surface area was calculated by the BET method. Pore size distribution was calculated by the BJH method. Transmission electron microscopy (TEM) morphologies of samples were observed on a Philips TEMCNAI−12 with an acceleration voltage of 100–120 kV. NH_3 temperature–programmed desorption (NH_3–TPD) profiles of the samples were carried out on a TP-5000 adsorption instrument made by Tianjin Xianquan Corporation (China). About 100 mg sample with particle sizes in a range of 240–425 μm was pretreated in helium gas at the flowing rate of 30 ml/min at 200 °C for 1 h. After that, the ammonia gas was adsorbed to saturation at room temperature following by flushing the samples with helium gas at 80 °C for 40 min until the integrator baseline was stable. NH_3–TPD curves were obtained at a heating rate of 10 °C/min from 100 to 700 °C. The TPD was measured with a TCD detector.

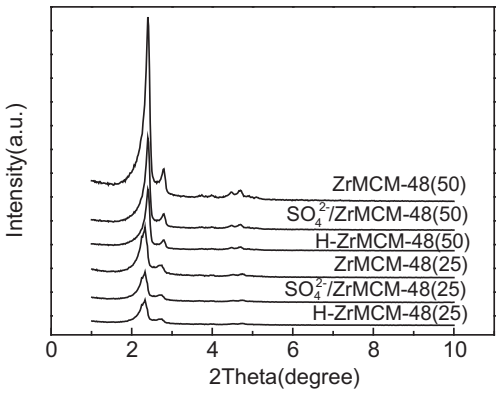

Figure 1 Low-angle XRD patterns of various samples.

2.7. Catalytic test

The alkylation of phenol with *tert*-butyl alcohol was carried out in a fixed-bed flow reactor (WFD-3030) with a stainless

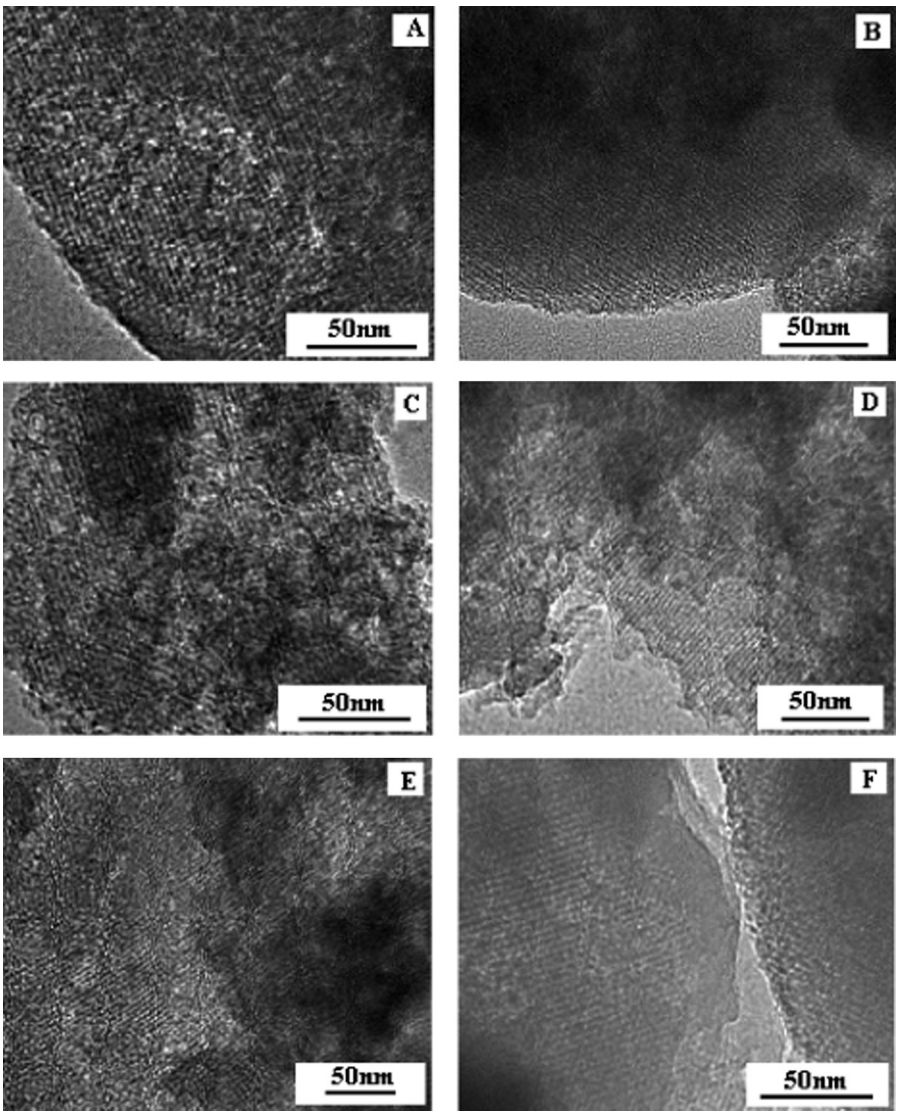

Figure 2 TEM images of various samples. (A) ZrMCM-48(50); (B) ZrMCM-48(25); (C)SO_4^{2-}/ZrMCM-48(50); (D) SO_4^{2-}/ZrMCM-48(25); (E) H-ZrMCM-48(50); (F) H-ZrMCM-48(25).

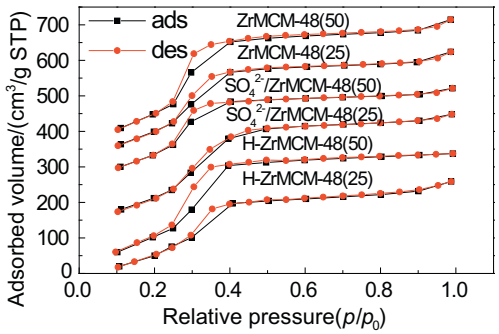

Figure 3 N_2 adsorption–desorption isotherms of various samples.

steel reaction tube. Before the start of the reaction, the catalysts were activated at 400 °C in air for 10 h followed by cooling to room temperature in nitrogen atmosphere. In a typical run, 500 mg of catalyst was placed in the reaction tube, and the reactant mixture, i.e., phenol and *tert*-butyl alcohol, was fed into the preheating reactor using a liquid injection pump (WMCB102-A) at a flowing rate of 60 ml/min using N_2 as the carrier gas. In this case, the preheating temperature was kept at 75 °C. After that, the preheated reactant mixture with a flowing nitrogen entered into the fixed-bed flow reactor to process alkylation reaction. The effluents were cooled to room temperature in air and collected at every 2 h interval. The products were analyzed by SP-2000 gas chromatograph fitted with a SE-54 capillary column coupled with FID.

3. Results and discussion

3.1. XRD analysis

The low-angle powder XRD patterns of the ZrMCM-48, SO_4^{2-}/ZrMCM-48 and H-ZrMCM-48 samples are shown in Fig. 1. It is observed that the ZrMCM-48(50) sample exhibits a high intensity diffraction peak (211) followed by a small peak (220) in the 2θ range of 2–3° and several diffraction peaks are also noted in the 2θ range of 3–6°, suggesting the formation of the typical *Ia3d* cubic mesoporous framework with high order. This is consistent with the results of the Refs. (Zhang et al., 2012; Zhao et al., 2010b). For ZrMCM-48 samples, an obvious decrease in the intensity of diffraction peak is seen with the increase in zirconium content, suggesting that the cubic mesoporous structure was partially collapsed. Besides, it can be noted from Fig. 1 that the SO_4^{2-}/ZrMCM-48 and H-ZrMCM-48 samples have obvious mesoporous characteristic peaks of MCM-48, showing that these samples still retained the cubic mesoporous framework, but the mesoporous ordering slightly deteriorated as compared with the parent ZrMCM-48 samples.

Table 1 Specific surface areas, average pore sizes and pore volumes of the samples.

Sample	Surface areas m^2/g	Average pore size nm	Pore volume cm^3/g
ZrMCM-48(50)	1246.99	2.50	0.92
ZrMCM-48(25)	1007.08	2.50	0.76
SO_4^{2-}/ZrMCM-48(50)	975.16	2.46	0.71
SO_4^{2-}/ZrMCM-48(25)	937.37	2.45	0.68
H-ZrMCM-48(50)	1059.33	2.45	0.85
H-ZrMCM-48(25)	724.02	2.74	0.61

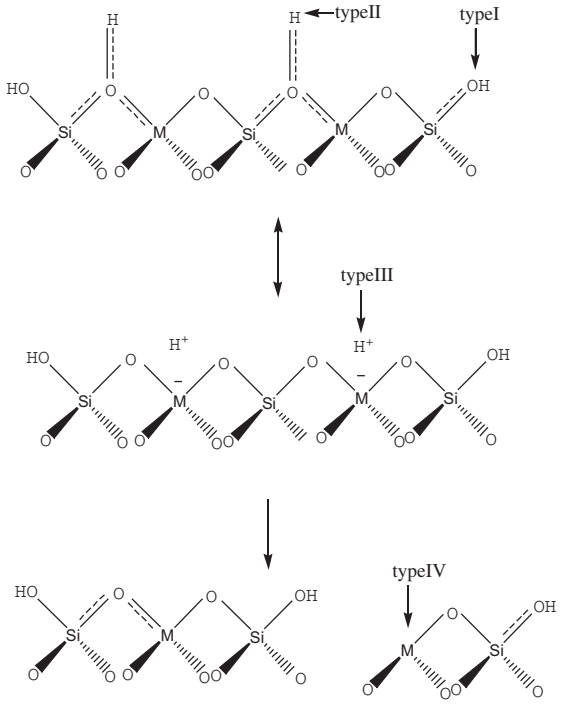

Scheme 1 Representation of the various acidic sites in M-MCM-48 (adapted from Dapurkar and Selvam, 2003).

3.2. TEM analysis

Fig. 2 presents the TEM images of various samples. Clearly, it can be noted that all samples exhibit a well-defined ordered mesoporous structure of MCM-48. At the same time, as shown in Fig. 2c–f, it was found that the mesoporous frameworks of the four solid acid catalysts were slightly damaged, but these catalysts still retained good mesoporous ordering. This further indicates that introduction of SO_4^{2-} or H^+ has little influence on mesoporous structures of ZrMCM-48 mesoporous molecular sieves.

3.3. Results of nitrogen physical adsorption

Fig. 3 illustrates the N_2 adsorption–desorption isotherms of all samples. As can be seen from Fig. 3, the isotherms in all cases exhibit the typical IV type adsorption isotherms with hysteresis loop, typical indication of mesoporous materials (Yang et al., 2005). A sharp inflection corresponding to the capillary condensation within uniform mesopores was observed in the relative pressure range of 0.25–0.4, which indicates that the SO_4^{2-}/ZrMCM-48 or H-ZrMCM-48 samples obtained after impregnation using H_2SO_4 or NH_4NO_3 solution still have typical mesoporous framework. Therefore, it can be concluded that there is no obvious influence on mesoporous structure of ZrMCM-48 samples after the introduction of SO_4^{2-} or H^+.

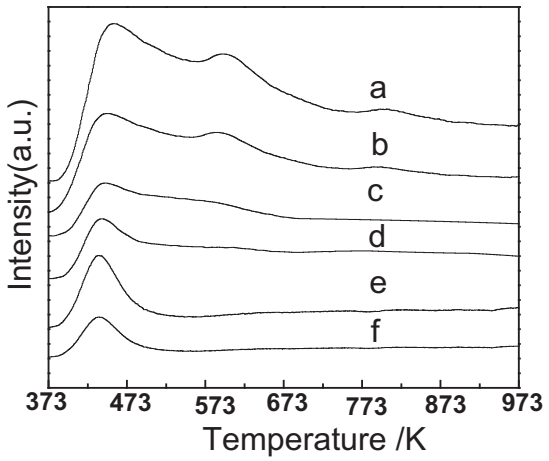

Figure 4 NH_3–TPD profiles of various samples. (a) SO_4^{2-}/ZrMCM-48(25); (b) SO_4^{2-}/ZrMCM-48(50); (c) H-ZrMCM-48(25); (d) H-ZrMCM-48(50); (e) ZrMCM-48(25); (f) ZrMCM-48(50).

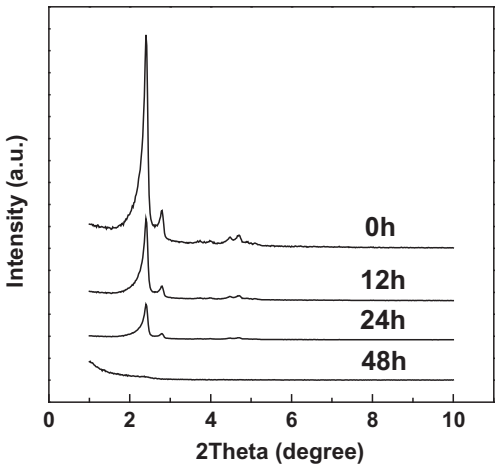

Figure 6 XRD patterns of the ZrMCM-48(50) sample after hydrothermal treatment at 100 °C for different time (0, 12, 24 and 48 h).

Table 1 listed the corresponding textural properties including the BET surface areas, BJH pore sizes and pore volumes. As shown in Table 1, we can see that the specific surface areas and pore volumes of the ZrMCM-48 samples decreased with the increase in Zr content, indicating that the higher Zr content deteriorated the mesoporous structure of ZrMCM-48 sample, which is in agreement with the analysis results of XRD. Further, the BET surface areas of the SO_4^{2-}/ZrMCM-48 or H-ZrMCM-48 samples decreased as compared with the parent ZrMCM-48 samples, suggesting that the mesoporous structures of these samples were slightly damaged. Combined with the analytic results of the N_2 adsorption–desorption isotherms, these samples still retained the cubic mesoporous structure of MCM-48. On the other hand, from Table 1, pore size can be seen in the range of 2.45–2.74 nm, indicating that these samples have the uniform pore size distribution.

3.4. NH_3–TPD analysis

The acid site distributions in H-ZrMCM-48 and SO_4^{2-}/ZrMCM-48 samples were determined by NH_3–TPD measurement. According to the Ref. (Dapurkar and Selvam, 2003; Sakthivel et al., 2000), the desorption peak around 423–443 K is due to surface hydroxyl groups from weak acid sites (type I); the two desorption peaks at the range of 453–483 K and 543–603 K originate from moderate and strong (Brönsted) acid sites that are aroused by the presence of metal element in two different framework positions, referred as type II and type III; the peak at 653–703 K may arise from tri-coordinated metal element in the framework, which is attributed to weak Lewis acid sites (type IV). A schematic representation of the various acidic sites is shown in Scheme 1.

The NH_3–TPD profiles of several samples at the temperature range from 373 to 973 K are depicted in Fig. 4. As shown in Fig. 4, the SO_4^{2-}/ZrMCM-48 and H-ZrMCM-48 samples all exhibited two NH_3 desorption peaks around 453 and 623 K. Besides, it is seen from Fig. 4 that the two SO_4^{2-}/ZrMCM-48 samples have one NH_3 desorption peak around 775 K. The desorption peak around *ca.* 453 K is due to surface hydroxyl groups (weak Brönsted acid sites, type I). The peak at about 623 K belongs to type III, originating from strong (Brönsted) acid sites. For SO_4^{2-}/ZrMCM-48 samples, the peak at 775 K is attributed to strong Lewis acid sites (Kosslick et al., 1998). Moreover, for the ZrMCM-48(25) and ZrMCM-48(50) samples, only one NH_3 desorption peak around 453 K

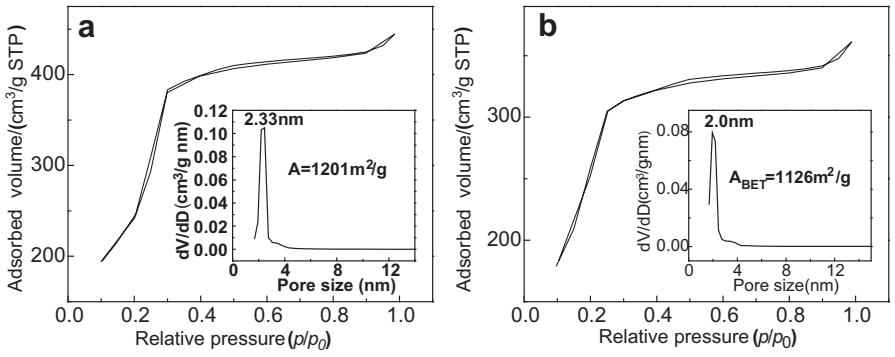

Figure 5 N_2 adsorption–desorption isotherms of the ZrMCM-48(50) sample after calcination at 700 (a) and 800 °C (b) for 4 h. The inset shows the BJH pore size distribution calculated from the desorption branch of the isotherm.

can be noted, showing that the two samples have certain number of weak acid sites and the strong acid sites are lacking. Further, we can also observe that with the increase in zirconium content, the area and intensity of the NH_3 desorption peak increase, indicating that the ZrMCM-48 with higher Zr content has much more weak acidic sites (see Fig. 4).

3.5. Thermal and hydrothermal stability test

Fig. 5 illustrates the N_2 adsorption–desorption isotherms of the ZrMCM-48(50) sample after calcination at 700 and 800 °C for 4 h as well as the pore size distribution curves (inset), respectively. The isotherms still maintained the type IV isotherms with a capillary condensation step even after the ZrMCM-48(50) sample was calcined at 800 °C for 4 h. Further, by comparing with the ZrMCM-48(50)-800, the isotherms of the ZrMCM-48(50)-700 sample exhibited a sharper step, showing that both of the samples have good mesoporous ordering. Their specific surface areas and pore sizes calculated by BET and BJH methods were 1201 and 1126 m^2/g, and 2.33 and 2.0 nm, respectively. This indicates that both of the samples possess high surface area and narrow pore size

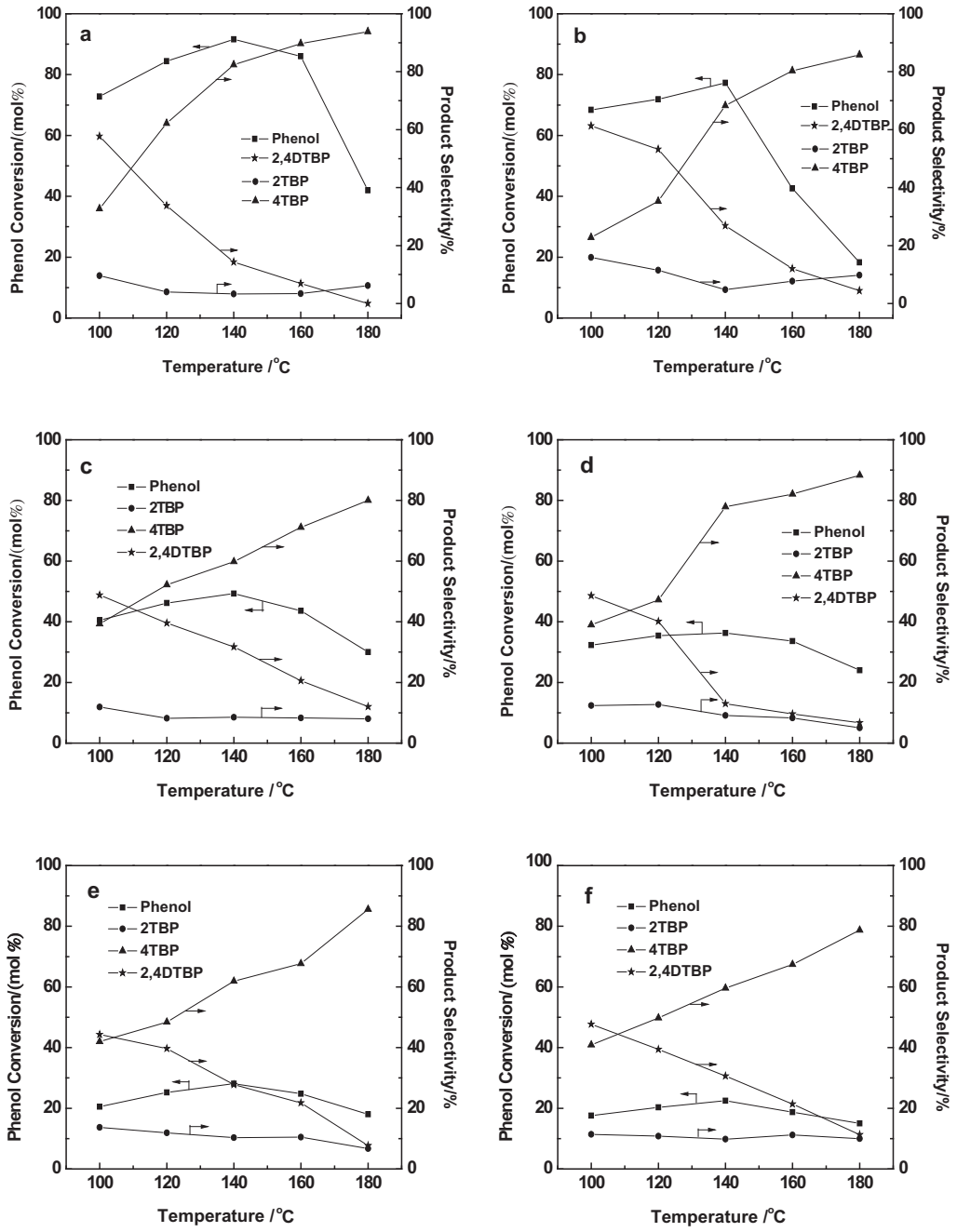

Figure 7 Phenol conversion and product selectivity over various catalysts at different reaction temperatures along with the optimum reaction conditions (WHSV = 2 h^{-1}, $n_{tert\text{-butanol}}/n_{phenol}$ = 2:1, time: 2 h). (a) SO_4^{2-}/ZrMCM-48(25); (b) SO_4^{2-}/ZrMCM-48(50); (c) H-ZrMCM-48(25); (d) H-ZrMCM-48(50); (e) ZrMCM-48(25); (f) ZrMCM-48(50).

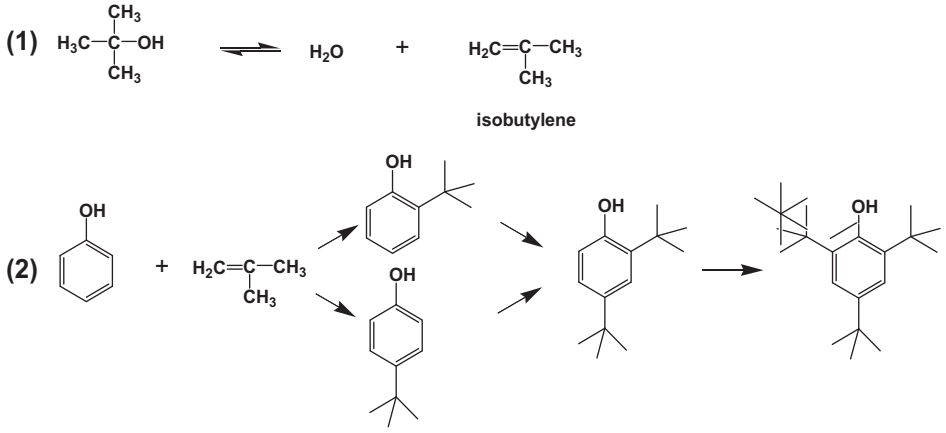

Scheme 2 A possible process of alkylation of phenol with *tert*-butyl alcohol.

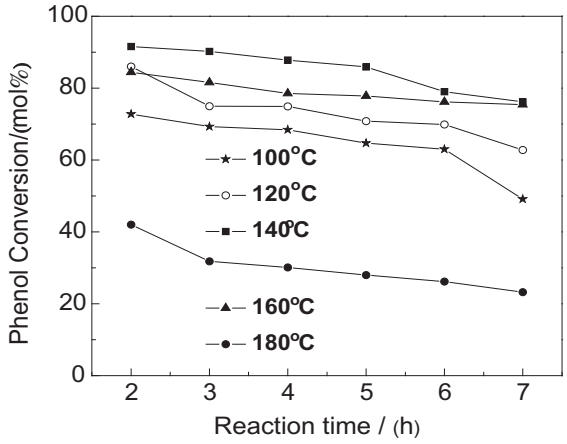

Figure 8 Effect of reaction time on phenol conversion over SO_4^{2-}/Zr-MCM-48–25 catalyst in the reaction temperature of 100–180 °C ($n_{tert\text{-butanol}}/n_{phenol}$ = 2:1, WHSV = 2 h^{-1}).

distribution, and the mesoporous structure was not significantly changed from calcination temperature of 800 °C, suggesting that the resulting ZrMCM-48(50)-800 sample has good thermal stability.

Fig. 6 presents the XRD patterns of the ZrMCM-48(50) sample after hydrothermal treatment at 100 °C for 0, 12, 24 and 48 h, respectively. It is noted that the characteristic diffraction peaks (211) and (220) existed obviously in the XRD pattern of the ZrMCM-48(50)-12 h sample, and the weak diffraction peaks (420) and (322) can be seen. It indicates that the cubic *Ia3d* mesoporous structure still retained after the ZrMCM-48(50) sample was hydrothermal treated at 100 °C for 12 h. However, as the hydrothermal treatment time increases to 24 h, the intensity of the diffraction peaks (211) and (220) became weak, and the diffraction peaks (420) and (322) disappeared, showing that the ordered mesoporous structure was partial loss, the mesoporous ordering deteriorated. When the hydrothermal treatment time increased to 48 h, the cubic mesoporous framework was completely collapsed. The intensity of basal peak (211) gradually decreased with an increase in hydrothermal treatment time, indicating that the ordering of ZrMCM-48 sample gradually degraded. It is reasonable to conclude that the resulting ZrMCM-48 sample possesses good hydrothermal stability.

3.6. Catalytic activity

3.6.1. Effect of reaction temperature on phenol conversion and product selectivity

The effect of different reaction temperatures on phenol conversion and product selectivity of alkylation of phenol with *tert*-butyl alcohol over various catalysts is shown in Fig. 7. According to Fig. 7, we found that the conversion of phenol over all catalysts increased with the increase in temperature from 100 to 140 °C, which may be attributed to the domination of the alkylation at lower temperature up to 140 °C, the phenol conversion reaches a maximum in all cases. Beyond this temperature, *viz*. at the temperature range of 140–180 °C, the conversion of phenol decreased with the increasing of reaction temperature. This behavior could be due to the fact that the speed of dealkylation reaction is faster than that of alkylation reaction at the higher temperature (Elavarasan et al., 2011). Additionally, it is noted that the phenol conversion is related to the Zr content in sample. For example, when SO_4^{2-}/ZrMCM-48 catalysts were respectively used in the alkylation reaction at 140 °C, the phenol conversions increased from 77.3% to 91.6% with the variation of the Si/Zr molar ratio from 50 to 25, implying that the solid acid catalyst with higher Zr content exhibits higher catalytic activity. This is probably attributed to an increase in amount of acid sites with an increase in Zr content (see Fig. 4). The related results obtained at other reaction temperatures are shown in Fig. 7. A similar trend was also observed over H-ZrMCM-48 solid acid catalysts. Further, it can be noted that the phenol conversion over the SO_4^{2-}/ZrMCM-48(25) catalyst is the highest among all catalysts and reaches 91.6%, suggesting that the SO_4^{2-}/ZrMCM-48(25) catalyst exhibits the highest catalytic activity. This is probably attributed to the amount of the strong acid sites for SO_4^{2-}/ZrMCM-48(25) which is much more than that of other catalysts (Savidha et al., 2004).

Moreover, as can be observed from Fig. 7 the major products over all catalysts are 4-TBP, 2-TBP and 2,4-DTBP, respectively. No 2,6-DTBP and 2,4,6-TTBP were observed. As the reaction temperature increased from 100 to 180 °C, the selectivity to 4-TBP increased while the selectivity to 2-TBP and 2,4-DTBP decreased. This may be due to the following reasons: the steric hindrance of 2-TBP increased with the increase in reaction temperature (Wu et al., 2006). The

Table 2 Catalytic performance of H-MCM-48 and H-Y for *tert*-butylation of phenol.

Catalyst	Conversion of phenol/wt%	Selectivity of products/wt%		
		2-TBP	4-TBP	2,4-DTBP
H-MCM-48	2.8	16.77	78.74	6.33
H-Y	81.02	5.55	69.58	22.46

Reaction condition: 0.5 g catalyst, n(*tert*-butanol)/n(phenol) = 2:1, time = 2 h, temperature = 140 °C, WHSV = 2 h^{-1}.

other one is that the dealkylation is dominant at higher temperature leading to the effortless formation of 4-TBP with low steric hindrance. A maximum selectivity to 4-TBP of 93.8% over SO_4^{2-}/ZrMCM-48(25) can be seen at 180 °C, and accompanied with the maximum selectivity to 2,4-DTBP of 57.7% at 100 °C, indicating that the higher temperature is favorable for the formation of 4-TBP and the 2,4-DTBP is easily formed at the lower temperature. Furthermore, according to the product distribution, a possible process for the alkylation reaction of phenol with *tert*-butyl alcohol over H-ZrMCM-48 (or SO_4^{2-}/ZrMCM-48) catalysts is shown in Scheme 2.

3.6.2. Effect of reaction time on catalytic activity

Fig. 8 depicts the effect of reaction time on phenol conversion over the SO_4^{2-}/ZrMCM-48(25) catalyst in the reaction temperature range of 100–180 °C. As shown in Fig. 8, it is noted that in the temperature range, the phenol conversion gradually decreased with the increase of reaction time from 2 to 7 h. This may be attributed to the deactivation of the catalyst aroused by longer contact time. After 7 h, we found that the phenol conversion reaches to 76.2%, indicating that the SO_4^{2-}/ZrMCM-48(25) catalyst still has high catalytic activity and suggesting that the SO_4^{2-} is slight loss before and after reaction.

3.7. Results of alkylation of phenol with butyl alcohol over H-MCM-48 and H-Y catalysts?

The results of alkylation of phenol with alcohol over H-MCM-48 and H-Y catalysts under the optimum reaction condition are listed in Table 2. From Table 2, we found that the phenol conversion over H-MCM-48 catalyst is only 2.8%. Although the phenol conversion over H-Y catalyst reaches 81.02%, the selectivity to 2,4-DTBP is lower than that of the H-ZrMCM-48 and SO_4^{2-}/ZrMCM-48. This may be due to the following: the microporous structure of H-Y catalyst limited the formation of 2,4-DTBP.

4. Conclusions

A series of SO_4^{2-}/ZrMCM-48 and H-ZrMCM-48 solid acid catalysts were successfully prepared *via* the wet impregnation method with H_2SO_4 and NH_4NO_3 solution, respectively. There is no obvious influence on mesoporous structure of MCM-48 after introducing of SO_4^{2-} or H^+ and these solid acid catalysts still retain the cubic mesoporous framework. In the alkylation of phenol with *tert*-butyl alcohol, the SO_4^{2-}/ZrMCM-48(25) catalyst was found to be the most promising and gave the highest phenol conversion among all catalysts. A maximum phenol conversion of 91.6% with 81.8% selectivity to 4-TBP was achieved when the molar ratio of *tert*-butyl alcohol: phenol is 2, the WHSV is 2 h^{-1}, the reaction time is 2 h and the reaction temperature is 140 °C.

Acknowledgements

This work was supported by National Nature Science Foundation of China (21004031) and Senior Personality Fund of Jiangsu University (12JDG106).

References

Anand, R., Maheswari, R., Gore, K.U., Tope, B.B., 2003. Tertiary butylation of phenol over HY and dealuminated HY zeolites. J. Mol. Catal. A: Chem. 193, 251–257.

Badamali, S.K., Sakthivel, A., Selvam, P., 2000. Tertiary butylation of phenol over mesoporous H-FeMCM-41. Catal. Lett. 65, 153–157.

Chandra, K.G., Sharma, M.M., 1993. Alkylation of phenol with MTBE and other tert-butylethers: cation exchange resins as catalysts. Catal. Lett. 19, 309–317.

Chen, F.T., Ma, H.Z., Wang, B., 2007. Cobalt modified solid superacid assisted electrochemical reaction of toluene with methanol. J. Hazard. Mater. 147, 964–970.

Dapurkar, S.E., Selvam, P., 2003. Mesoporous H-AlMCM-48: highly efficient solid acid catalyst. Appl. Catal. A: Gen. 254, 239–249.

Du, E., Yu, S.M., Zuo, L.M., Zhang, J.S., Huang, X.Q., Wang, Y., 2011. Pb (II) sorption on molecular sieve analogues of MCM-41 synthesized from kaolinite and montmorillonite. Appl. Clay Sci. 51, 94–101.

Dumitriu, E., Hulea, V., 2003. Effects of channel structures and acid properties of large-pore zeolites in the liquid-phase *tert*-butylation of phenol. J. Catal. 218, 249–257.

Elavarasan, P., Kondamudi, K., Upadhyavula, S., 2011. Kinetics of phenol alkylation with tert-butyl alcohol using sulfonic acid functional ionic liquid catalysts. Chem. Eng. J. 166, 340–347.

Gui, J., Ban, H., Cong, X., Zhang, X., Hu, Z., Sun, Z., 2008. Selective alkylation of phenol with tert-butyl alcohol catalyzed by Brönsted acidic imidazolium salts. J. Mol. Catal. A: Chem. 225, 27–31.

Huang, J.H., Xing, L.H., Wang, H.S., Li, G., Wu, S.J., Wu, T.H., Kan, Q.B., 2006. Tertiary butylation of phenol over hexagonal *p6mm* mesoporous aluminosilicates with enhanced acidity. J. Mol. Catal. A: Chem. 259, 84–90.

Jiang, T.S., Zhao, Q., Li, M., Yin, H.B., 2008. Preparation of mesoporous titania solid superacid and tis catalytic property. J. Hazard. Mater. 159, 204–209.

Jiang, T.S., Wu, D.L., Song, J.N., Zhou, X.P., Zhao, Q., Ji, M.R., Yin, H.B., 2011. Synthesis and characterization of mesoporous ZrMCM-48 molecular sieves with good thermal and hydrothermal stability. Powder Technol. 207, 422–427.

Kosslick, H., Lischke, G., Landmesser, H., Parlitz, B., Storek, W., Fricke, R., 1998. Acidity and catalytic behavior of substituted MCM-48. J. Catal. 176, 102–114.

Kresge, C.T., Leonowicz, M.E., Roth, W.J., Vartuli, J.C., Beck, J.S., 1992. Ordered mesoporous molecular sieves synthesized by a liquid-crystal template mechanism. Nature 359, 710–712.

Krishnan, A.V., Ojha, K., Pradhan, N.C., 2002. Alkylation of phenol with tertiary butyl alcohol over zeolites. Org. Process Res. Dev. 6, 132–137.

Li, Y.G., Xue, B., Yang, Y.T., 2009. Synthesis of ethylbenzene by alkylation of benzene with diethyl oxalate over HZSM-5. Fuel Process. Technol. 90, 1220–1225.

Mathew, T., Rao, B.S., Gopinath, C.S., 2004. Tertiary butylation of phenol on $Cu_{1-x}Co_xFe_2O_4$: catalysis and structure–activity correlation. J. Catal. 222, 107–116.

Ojha, K., Pradhan, N.C., Samanta, A.C., 2005. Kinetics of batch alkylation of phenol with *tert*-butyl alcohol over a catalyst synthesized from coal fly ash. J. Chem. Eng. 112, 109–115.

Ronchin, L., Vavasori, A., Toniolo, L., 2012. Acid catalyzed alkylation of phenols with cyclohexene: comparison between homogeneous and heterogeneous catalysis, influence of cyclohexyl phenyl ether equilibrium and of the substituent on reaction rate and selectivity. J. Mol. Catal. A: Chem. 355, 134–141.

Sakthivel, A., Badamali, S.K., Selvam, P., 2000. Para-selective t-butylation of phenol over mesoporous H-AlMCM-41. Microporous Mesoporous mater. 39, 457–463.

Sakthivel, A., Dapurkar, S.E., Gupta, N.M., Kulshreshtha, S.K., Selvam, P., 2003. The influence of aluminium sources on the acidic behavior as well as on the catalytic activity of mesoporous H-AlMCM-41 molecular sieves. Microporous Mesoporous Mater. 65, 177–187.

Savidha, R., Pandurangan, A., Palanihamy, M., Murugesan, V., 2004. A comparative study on the catalytic activity of Zn and Fe containing Al-MCM-41 molecular sieves on t-butylation of phenol. J. Mol. Catal. A:Chem. 211, 165–177.

Sohn, J.R., Lee, S.H., Lim, J.S., 2006. New solid superacid catalyst prepared by doping ZrO_2 with Ce and modifying with sulfate and its catalytic activity for acid catalysis. Catal. Today 116, 143–150.

Subashini, D., Pandurangan, A., 2007. Synthesis of mesoporous molecular sieves as catalytic template for the growth of single walled carbon nanotubes. Catal. Commun. 8, 1665–1770.

Subrahmanyam, C.H., Viswanathan, B., Varadarajan, T.K., 2005. Alkylation of naphthalene with alcohols over acidic mesoporous solids. J. Mol. Catal. A: Chem. 226, 155–163.

Vinu, A., Usha Nandhini, K., Murugesan, V., Böhlmann, W., Umamaheswari, V., Pöppl, A., Hartmann, M., 2004. Mesoporous FeAlMCM-41: an improved catalyst for the vapor phase *tert*-butylation of phenol. Appl. Catal. A 265, 1–10.

Wu, S.J., Huang, J.H., Wu, T.H., Song, K., Wang, H.S., Xing, L.H., Xu, H.Y., Xu, L., Guan, J.Q., Kan, Q.B., 2006. Synthesis, characterization, and catalytic performance of mesoporous Al-SBA-15 for tert-butylation of phenol. Chin. J. Catal. 27, 9–14.

Yadav, G.D., Pathre, G.S., 2006. Novel mesoporous for selective C-alkylation of m-cresol with tert-butanol. Microporous Mesoporous Mater. 89, 16–24.

Yang, X.L., Dai, W.L., Gao, R.H., Chen, H., Li, H.X., Cao, Y., Fan, K.N., 2005. Synthesis, characterization and catalytic application of mesoporous W-MCM-48 for the selective oxidation of cyclopentene to glutaraldehyde. J. Mol. Catal. A: Chem. 241, 205–214.

Zhang, K., Yuan, E.H., Xu, L.L., Xue, Q.S., Luo, C., Albela, B., Bonneviot, L., 2012. Preparation of high-quality MCM-48 mesoporous silica and the mode of action of the template. Eur. J. Inorg. Chem. 26, 4183–4189.

Zhao, Z.K., Wang, W.L., Qiao, W.H., Wang, G.R., Li, Z.S., Cheng, L.B., 2006. HY zeolite catalyst for alkylation of a-methylnaphthalene with long-chain alkenes. Microporous Mesoporous Mater. 93, 164–170.

Zhao, W., Li, Q.Z., Wang, L.N., Chu, J.L., Qu, J.K., Li, S.H., Qi, T., 2010a. Synthesis of high quality MCM-48 with binary cationic-nonionic surfactants. Langmuir 26, 6982–6988.

Zhao, D., Rodriguez, A., Dimitrijevic, N., Rajh, T., Koodali, R.T., 2010b. Synthesis, structural characterization, and photocatalytic performance of mesoporous W-MCM-48. J. Phys. Chem. C 114, 15728–15734.